



**QUEEN'S
UNIVERSITY
BELFAST**

Impact of primary networks on the performance of energy harvesting cognitive radio networks

Zhang, J., Nguyen, N-P., Zhang, J., Garcia-Palacios, F., & Ngoc, P. L. (2016). Impact of primary networks on the performance of energy harvesting cognitive radio networks. *IET Communications*. <https://doi.org/10.1049/iet-com.2016.0400>

Published in:
IET Communications

Document Version:
Peer reviewed version

Queen's University Belfast - Research Portal:
[Link to publication record in Queen's University Belfast Research Portal](#)

General rights

Copyright for the publications made accessible via the Queen's University Belfast Research Portal is retained by the author(s) and / or other copyright owners and it is a condition of accessing these publications that users recognise and abide by the legal requirements associated with these rights.

Take down policy

The Research Portal is Queen's institutional repository that provides access to Queen's research output. Every effort has been made to ensure that content in the Research Portal does not infringe any person's rights, or applicable UK laws. If you discover content in the Research Portal that you believe breaches copyright or violates any law, please contact openaccess@qub.ac.uk.

Impact of Primary Networks on the Performance of Energy Harvesting Cognitive Radio Networks

Jinghua Zhang, Nam-Phong Nguyen, Junqing Zhang, Emiliano Garcia-Palacios,
and Ngoc Phuc Le

Abstract

In this paper, we investigate the effect of the primary network on the secondary network when harvesting energy in cognitive radio in the presence of multiple power beacons and multiple secondary transmitters. In particular, the influence of the primary transmitter's transmit power on the energy harvesting secondary network is examined by studying two scenarios of primary transmitter's location, i.e., the primary transmitter's location is near to the secondary network, where the primary transmitter can interfere the secondary receiver, and the primary transmitter's location is far from the secondary network, where the secondary receiver is free from the interference. In addition, the peak interference constraint at the primary receiver is also considered. In the scenario where the primary transmitter locates near to the secondary network, although secondary transmitter can benefit from the harvested energy from the primary transmitter, the interference caused by the primary transmitter suppresses the secondary network performance. Meanwhile, in both scenarios, despite the fact that the transmit power of the secondary transmitter can be improved by the support of powerful power beacons, the peak interference constraint at the primary receiver limits this advantage. In addition, the deployment of multiple power beacons and multiple secondary transmitters can improve the performance of the secondary network. The analytical expressions of the outage probability of the secondary network in the two scenarios are also provided and verified by numerical simulations.

J. Zhang, N.-P. Nguyen, J. Zhang, and E. Garcia-Palacios are with Queen's University Belfast, UK (email: {jzhang22, pnguyen04, jzhang20}@qub.ac.uk. and e.garcia@ee.qub.ac.uk).

N. P. Le is with Duy Tan University, Vietnam (email: phucln81@yahoo.com).

This work was supported by the Newton Institutional Link under Grant ID 172719890.

I. INTRODUCTION

In some wireless communication networks (such as wireless sensor networks), energy restrains the performance of the networks. Prolonging the lifetime of these networks has many difficulties since replacing or recharging energy suppliers of the nodes is either inconvenient or undesirable. In these situations, energy harvesting (EH) has become a promising technique to power energy-constrained wireless networks and recently attracted a great deal of attention [1]–[3]. The main idea is that a wireless node is equipped with rectifying circuits that can convert the the radio frequency (RF) signal sent by power source nodes into DC current. This current is saved into batteries for serving signal processing and transmission. In practice, wireless EH has not been widely used because of the high propagation loss of RF signals. However, thanks to the latest developments in wireless communications, i.e., small cells [4], large-scale antenna arrays [5], millimetre-wave communications [6], the transmission efficiency is significantly increased, which will significantly decrease the propagational loss and obtain much higher EH efficiencies [7]. Furthermore, users' energy consumption will be continuously reduced by the advancements in low-power electronics [8]. Therefore, RF EH has a great potential to be widely implemented in the next-generation wireless communication systems. In [9] and [10], the authors considered the scenarios where the destination simultaneously receives wireless information and harvests wireless power from the source. Motivated by these works, in [11]–[13], the author studied performance of wireless systems that are applied EH. These studies have laid a solid foundation for understanding the role of EH in wireless communication networks.

The booming in the growth of wireless devices and services has brought enormous request of spectrum resources while most of the licensed spectrum bands are occupied [14]. Under this circumstance, it is urgent to deploy new technologies that have the abilities of optimizing the current spectrum usage and adapting to the present spectrum management policies. Fortunately, to tackle these challenges, cognitive radio (CR) was introduced in [15], [16]. In CR networks, the unlicensed users are allowed to transfer messages over the licensed spectrum under the constraint that the interference level at the primary users is kept below a harmless threshold [17]. Therefore, reliable communication can be established without considering the secondary networks' operation [18].

The combination of CR and EH technologies can bring great advantages to wireless communication networks. This topic has been received wide attention recently. In [19], the authors

proposed a centralized channel access strategy for a multichannel low-power CR system, where the SUs can employ a unused spectrum band for either harvesting RF energy from PUs' transmission or transmitting their information. In [20], an EH-CR system was investigated, in which the secondary users using the harvested energy for transmission after harvesting energy from ambient radio signal. The authors in [21] considered finite batteries EH-CR systems where the SUs can be configured to improve PU detecting and PU spectrum opportunistically utilizing process. However, the impact of primary network on the secondary network in the EH-CR context has not been well-investigated.

In this paper, we propose an EH-CR network in the presence of multiple multi-antenna power beacons and multiple secondary transmitters. The contribution of this paper is summarized as follows:

- We propose an EH-CR network in which multiple multi-antenna power beacons are deployed to power secondary transmitters and a secondary transmitter selection scheme based on the channel state information (CSI) of the secondary network is investigated. In addition, we study the effect of primary transmitter on the secondary network by considering two scenarios of the primary transmitter's location, e.g., the primary transmitter is located near to the secondary network and the primary transmitter is located far from the secondary network.
- We develop the analytical expressions to investigate the effect of the primary network on the secondary network in the two scenarios of primary transmitter's location with respect to the primary transmitter's transmit power and the peak interference constraint at the primary receiver.
- We demonstrate that in the case of near primary transmitter, although secondary transmitters can benefit from the harvested energy from primary transmitter, the interference caused by the primary transmitter suppresses the secondary network performance. Meanwhile, the peak interference constraint at the primary receiver limits the advantage that powerful power beacons can bring to the secondary transmitter. Besides, increasing the number of power beacons and secondary transmitter can improve the performance of the secondary network.

II. SYSTEM AND CHANNEL MODELS

We consider an EH-CR network consisting of one primary transmitter P_{TX} , one primary receiver P_{RX} , N power beacons B_n for $n = 1...N$, M secondary transmitters S_m for $m = 1...M$,

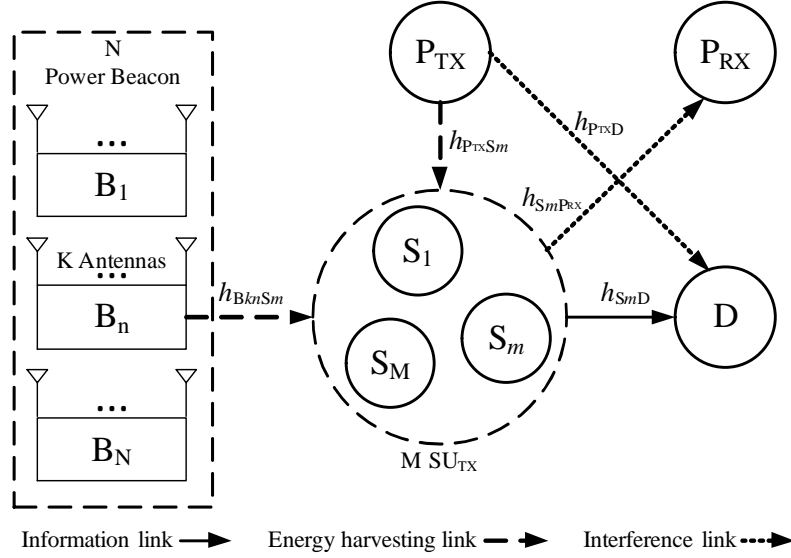


Fig. 1: System model.

and one secondary receiver D as shown in Fig. 1. The power beacons are equipped with K antennas while the other nodes are equipped with one antenna. In this work, we assume that all the nodes are located sufficiently far from each other so that all the channels experience independent and identically distributed Rayleigh fading. In this network, one secondary transmitter S_s will be selected from the M S_m to transmit information to D. The motivation of this scheme is that in wireless sensor networks, some of sensor nodes form a cluster that can exchange information among nodes. To save energy, one node in the cluster that has the best link to the sink will be chosen to transmit information to the sink. The selection is based on the CSI of the $S_m \rightarrow D$ link as follows:

$$|h_{S_sD}|^2 = \max_{m=1 \dots M} [|h_{S_mD}|^2], \quad (1)$$

where $|h_{S_sD}|^2$ and $|h_{S_mD}|^2$ are the channel power gains from the chosen secondary transmitter and S_m to D, respectively. The selection process can be done by using feedback channels from D to S_m . After the secondary transmitter selection process, S_s harvests RF energy by implementing time-switching based architecture shown in Fig. 2 while other secondary transmitters enter the idle mode. In a transmission block time T , S_s uses τT to harvest energy (EH phase) and $(1-\tau)T$ to transmit information to D (transmission phase), where $1 > \tau > 0$. In EH phase, to maximize

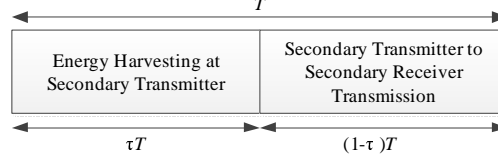


Fig. 2: Time switching based energy harvesting protocol.

the harvested energy at the selected transmitter, all the power beacons deploy beamforming technique to transmit power signal to S_s . In this paper, we consider two scenarios of P_{TX} 's location, i.e., i) P_{TX} is near to secondary network (NP) and ii) P_{TX} is far from the secondary network (FP).

A. P_{TX} is near to the secondary network

In this scenario, P_{TX} is located near the secondary network. Therefore, S_s can harvest energy from B and P_{TX} . However, the primary network's signal transmitted from P_{TX} can interfere D. The energy harvested at the S_s can be formulated as

$$E_s^{NP} = \eta \tau T \left(\frac{\mathcal{P}_B}{K} \sum_{k=1}^K \sum_{n=1}^N |h_{B_{n,k}S_s}|^2 + \mathcal{P}_{P_{TX}} |h_{P_{TX}S_s}|^2 \right), \quad (2)$$

where $0 < \eta < 1$ is the conversion efficiency coefficient and depends on the AC-DC converter circuit, \mathcal{P}_B is the transmit power of B_n , $\mathcal{P}_{P_{TX}}$ is the transmit power of P_{TX} , $|h_{B_{n,k}S_s}|^2$ is the channel power gain of the k -th antenna at the n -th power beacon to S_s link, and $|h_{P_{TX}S_s}|^2$ is the channel power gain of $P_{TX} \rightarrow S_s$ link. In the transmission phase, to protect the primary network, the transmit power of S_m must satisfy the maximal interference constraint \mathcal{I}_p at the primary receiver P_{RX} . The transmit power of S_s is given as

$$\mathcal{P}_{S_s}^{NP} = \min \left[\frac{E_s^{NP}}{(1-\tau)T}, \frac{\mathcal{I}_p}{|h_{S_sP_{RX}}|^2} \right], \quad (3)$$

where the coefficient $(1-\tau)T$ indicates that S_s uses the harvested energy to transmit information to D in the transmission phase, and $|h_{S_sP_{RX}}|^2$ is the channel power gain of $S_s \rightarrow P_{RX}$ link. At the secondary receiver, the information signal from S_m is interfered by the signal from the P_{TX} and the additive white Gaussian noise (AWGN). The received signal at D is given as

$$y_D = \sqrt{\mathcal{P}_{S_s}^{NP}} h_{S_sD} x_{S_sD} + \sqrt{\mathcal{P}_{P_{TX}}} h_{P_{TX}D} x_{P_{TX}D} + \sigma, \quad (4)$$

where $h_{S_s D}$ is the channel coefficient of $S_s \rightarrow D$ link, $h_{P_{TX} D}$ is the channel coefficient of $P_{TX} \rightarrow D$ link, $x_{S_s D}$ is the desired signal from S_s to D , $x_{P_{TX} D}$ is the interference signal from primary network, and σ is the AWGN at D with zero mean and N_0 variance. The signal to interference plus noise ratio (SINR) at D is given as

$$\Psi_D^{NP} = \frac{\mathcal{P}_{S_s}^{NP} |h_{S_s D}|^2}{N_0 + \mathcal{P}_{P_{TX}} |h_{P_{TX} D}|^2} = \frac{\gamma_S^{NP} |h_{S_s D}|^2}{1 + \gamma_P |h_{P_{TX} D}|^2}, \quad (5)$$

where $\gamma_P = \frac{\mathcal{P}_{P_{TX}}}{N_0}$ and γ_S^{NP} can be written as

$$\begin{aligned} \gamma_S^{NP} &= \min \left(\frac{E_s^{NP}}{N_0(1-\tau)T}, \frac{\mathcal{I}_p}{N_0 |h_{S_s P_{RX}}|^2} \right) \\ &= \min \left(\frac{\gamma_B \alpha}{K} \sum_{k=1}^K \sum_{n=1}^N |h_{B_{n,k} S_s}|^2 + \gamma_P \alpha |h_{P_{TX} S_s}|^2, \frac{\gamma \mathcal{I}_p}{|h_{S_s P_{RX}}|^2} \right), \end{aligned} \quad (6)$$

where $\gamma_B = \frac{\mathcal{P}_B}{N_0}$, $\gamma \mathcal{I}_p = \frac{\mathcal{I}_p}{N_0}$, and $\alpha = \frac{\eta \tau}{1-\tau}$.

B. P_{TX} is far from the secondary network

In this scenario, P_{TX} is located far from the secondary network. Therefore, S_s can not harvest energy from P_{TX} and D is free from P_{TX} 's interference. The energy harvested at the S_s can be formulated as

$$E_s^{FP} = \frac{\mathcal{P}_B \eta \tau T}{K} \sum_{k=1}^K \sum_{n=1}^N |h_{B_{n,k} S_s}|^2. \quad (7)$$

The transmit power of S_s is given as

$$\mathcal{P}_{S_s}^{FP} = \min \left[\frac{E_s^{FP}}{(1-\tau)T}, \frac{\mathcal{I}_p}{|h_{S_s P_{RX}}|^2} \right], \quad (8)$$

The received signal at D is given as

$$y_D = \sqrt{\mathcal{P}_{S_s}^{FP}} h_{S_s D} x_{S_s D} + \sigma, \quad (9)$$

The SNR at D is given as

$$\Psi_D^{FP} = \frac{\mathcal{P}_{S_s}^{FP} |h_{S_s D}|^2}{N_0} = \gamma_S^{FP} |h_{S_s D}|^2, \quad (10)$$

where $\gamma_S^{FP} = \min \left(\frac{\gamma_B \alpha}{K} \sum_{k=1}^K \sum_{n=1}^N |h_{B_{n,k} S_s}|^2, \frac{\gamma \mathcal{I}_p}{|h_{S_s P_{RX}}|^2} \right)$.

III. OUTAGE PROBABILITY

In this section, we analyse the outage probability (OP) of the considered system. The channel capacity of $S_s \rightarrow D$ link is given as

$$C_{\mathcal{M}} = (1 - \tau) \log_2 (1 + \Psi_D), \quad (11)$$

where the coefficient $(1 - \tau)$ indicates that the transmission duration of the source node is $(1 - \tau)T$ of the total block time T . The OP of the considered system is the probability that channel capacity of $S_s \rightarrow D$ link is smaller than a target rate. The OP can be formulated as

$$\begin{aligned} \mathbb{P}_{\text{out}} &= \mathbb{P} \{C_{\mathcal{M}} < R_{th}\} \\ &= \mathbb{P} \{\Psi_D < \beta\} \\ &= F_{\Psi_D}(\beta), \end{aligned} \quad (12)$$

where R_{th} is the target rate of the considered network, $\beta = 2^{\frac{R_{th}}{1-\tau}} - 1$, and $F_{\Psi_D}(x)$ is the cumulative distribution function (CDF) of Ψ_D .

A. P_{TX} is near to the secondary network

To facilitate finding the CDF of Ψ_D^{NP} , we denote

$$\begin{aligned} \mathcal{A} &= \frac{\gamma_B \alpha}{K} \sum_{k=1}^K \sum_{n=1}^N |h_{B_{n,k} S_s}|^2 + \gamma_P \alpha |h_{P_{TX} S_s}|^2, \\ \mathcal{B} &= |h_{S_s P_{RX}}|^2, \\ \mathcal{Z} &= |h_{S_s D}|^2, \\ \mathcal{Y} &= \gamma_P |h_{P_{TX} D}|^2. \end{aligned} \quad (13)$$

The SNR at D can be rewritten as

$$\Psi_D^{\text{NP}} = \frac{\min(\mathcal{A}, \frac{\gamma_{I_P}}{\mathcal{B}}) \mathcal{Z}}{1 + \mathcal{Y}}. \quad (14)$$

\mathcal{Z} , \mathcal{Y} , and \mathcal{B} are exponential random variables. Therefore, the CDF of \mathcal{Z} , \mathcal{Y} , and \mathcal{B} are given respectively as follows:

$$F_{\mathcal{Z}}(z) = 1 - \sum_{m=1}^M \binom{M}{m} (-1)^{m+1} \exp\left(\frac{-mz}{\Omega_{SD}}\right), \quad (15)$$

$$F_{\mathcal{Y}}(y) = 1 - \exp\left(\frac{-y}{\gamma_P \Omega_{P_{TX} D}}\right), \quad (16)$$

$$F_{\mathcal{B}}(x) = 1 - \exp\left(\frac{-x}{\Omega_{SP_{RX}}}\right), \quad (17)$$

where Ω_{SD} , $\Omega_{P_{TX}D}$, and $\Omega_{SP_{RX}}$ are the average power gains of $S_s \rightarrow D$, $P_{TX} \rightarrow D$, and $S_s \rightarrow P_{RX}$ links, respectively. From the CDF of \mathcal{Y} and \mathcal{B} , the PDF of \mathcal{Y} and \mathcal{B} are respectively given as

$$f_{\mathcal{Y}}(y) = \frac{1}{\gamma_P \Omega_{P_{TX}D}} \exp\left(\frac{-y}{\gamma_P \Omega_{P_{TX}D}}\right), \quad (18)$$

$$f_{\mathcal{B}}(x) = \frac{1}{\Omega_{SP_{RX}}} \exp\left(\frac{-x}{\Omega_{SP_{RX}}}\right). \quad (19)$$

The PDF of \mathcal{A} is given as

$$f_{\mathcal{A}}(x) = \sum_{l=1}^{NK} \kappa_{1l} x^{l-1} \exp\left(\frac{-Kx}{\gamma_B \alpha \Omega_{BS}}\right) + \kappa_2 \exp\left(\frac{-x}{\gamma_P \alpha \Omega_{P_{TX}S}}\right), \quad (20)$$

where

$$\begin{aligned} \kappa_{1l} &= \frac{-(\gamma_P \alpha \Omega_{P_{TX}S})^{NK-l} K^{NK}}{\Gamma(l)(\gamma_B \alpha \Omega_{BS})^{l-1} (K \gamma_P \alpha \Omega_{P_{TX}S} - \gamma_B \alpha \Omega_{BS})^{KN-l+1}}, \\ \kappa_2 &= \frac{(\gamma_P \alpha \Omega_{P_{TX}S})^{KN-1} (-K)^{KN}}{(K \gamma_P \alpha \Omega_{P_{TX}S} - \gamma_B \alpha \Omega_{BS})^{KN}}. \end{aligned}$$

Proof: The proof is given in Appendix A. ■

From (15) and (18)-(20), we have the following lemma.

Lemma 1: The OP of the secondary network with neighbouring P_{TX} is given as follows:

$$\begin{aligned} \mathbb{P}_{\text{out}}^{\text{NP}} &= 1 - \sum_{m=1}^M \sum_{l=1}^{KN} \binom{M}{m} (-1)^{m+1} 2 \kappa_{1l} \left(\frac{m \gamma_B \alpha \beta \Omega_{BS}}{K \Omega_{SD}} \right)^{\frac{l}{2}} K_l \left(2 \sqrt{\frac{m K \beta}{\gamma_B \alpha \Omega_{SD} \Omega_{BS}}} \right) \\ &\quad - \sum_{m=1}^M \binom{M}{m} (-1)^{m+1} 2 \kappa_2 \sqrt{\frac{m \beta \gamma_P \alpha \Omega_{P_{TX}S}}{\Omega_{SD}}} K_1 \left(2 \sqrt{\frac{m \beta}{\gamma_P \Omega_{P_{TX}S} \Omega_{SD}}} \right) \\ &\quad - \sum_{m=1}^M \sum_{l=1}^{KN} \binom{M}{m} (-1)^m 2 \kappa_{1l} \left(\vartheta_m \Omega_{BS} \frac{\gamma_B \alpha}{K} \right)^{\frac{l}{2}} K_l \left(2 \sqrt{\frac{K \vartheta_m}{\gamma_B \alpha \Omega_{BS}}} \right) \\ &\quad - \sum_{m=1}^M \binom{M}{m} (-1)^m 2 \kappa_2 \sqrt{\vartheta_m \gamma_P \alpha \Omega_{P_{TX}S}} K_1 \left(2 \sqrt{\frac{\vartheta_m}{\gamma_P \alpha \Omega_{P_{TX}S}}} \right) \\ &\quad - \sum_{m=1}^M \sum_{l=1}^{KN} (-1)^m \kappa_{1l} \varrho_m \left[\Theta_1 \left(l-1, \varrho_m, \frac{m \beta}{\Omega_{SD}}, \frac{K}{\gamma_B \alpha \Omega_{BS}} \right) - \Theta_1 \left(l-1, \varrho_m, \vartheta_m, \frac{K}{\gamma_B \alpha \Omega_{BS}} \right) \right] \\ &\quad - \sum_{m=1}^M (-1)^m \kappa_2 \varrho_m \left[\Theta_2 \left(\varrho_m, \frac{m \beta}{\Omega_{SD}}, \frac{1}{\gamma_P \alpha \Omega_{P_{TX}S}} \right) - \Theta_2 \left(\varrho_m, \vartheta_m, \frac{1}{\gamma_P \alpha \Omega_{P_{TX}S}} \right) \right] \\ &\quad - \sum_{m=1}^M \sum_{l=1}^{KN} \binom{M}{m} \frac{(-1)^m \kappa_{1l} \gamma_{\mathcal{I}_p} \Omega_{SD} \exp(\varsigma_m)}{m \gamma_P \Omega_{SP_{RX}} \Omega_{P_{TX}D} \beta} \Theta_3 \left(l-1, \frac{K}{\gamma_B \alpha \Omega_{BS}}, \varsigma_m \gamma_{\mathcal{I}_p}, \frac{\varsigma_m \gamma_{\mathcal{I}_p} \Omega_{SD}}{m \gamma_P \Omega_{P_{TX}D} \beta} \right) \\ &\quad - \sum_{m=1}^M \binom{M}{m} \frac{(-1)^m \gamma_{\mathcal{I}_p} \Omega_{SD} \kappa_2 \exp(\varsigma_m)}{m \gamma_P \Omega_{SP_{RX}} \Omega_{P_{TX}D} \beta} \Theta_4 \left(\frac{1}{\gamma_P \alpha \Omega_{P_{TX}S}}, \varsigma_m \gamma_{\mathcal{I}_p}, \frac{\varsigma_m \gamma_{\mathcal{I}_p} \Omega_{SD}}{m \gamma_P \Omega_{P_{TX}D} \beta} \right), \quad (21) \end{aligned}$$

where $\varrho_m = \frac{m\gamma_P\Omega_{P_{TX}}\beta}{\Omega_{SD}}$, $\vartheta_m = \frac{m\beta}{\Omega_{SD}} + \frac{\gamma_{\mathcal{I}_p}}{\Omega_{SP_{RX}}}$, $\varsigma_m = \frac{m\beta\Omega_{SP_{RX}} + \gamma_{\mathcal{I}_p}\Omega_{SD}}{\gamma_{\mathcal{I}_p}\Omega_{SD}\Omega_{SP_{RX}}}$, $K_x(\cdot)$ defined in [22, Eq. (8.407.1)] is the modified Bessel function of the second kind, and

$$\begin{aligned}\Theta_1(a, b, c, d) &= \int_0^\infty \frac{y^a}{b+y} \exp\left(\frac{-c}{y} - dy\right) dy \text{ with } (a \geq 0, b > 0, c > 0, d > 0), \\ \Theta_2(a, b, c) &= \int_0^\infty \frac{1}{a+y} \exp\left(\frac{-b}{y} - cy\right) dy \text{ with } (a > 0, b > 0, c > 0), \\ \Theta_3(a, b, c, d) &= \int_0^\infty y^a \exp\left(\frac{-y}{b}\right) \text{Ei}\left(\frac{-c}{y} - d\right) dy \text{ with } (a \geq 0, b > 0, c > 0, d > 0), \\ \Theta_4(a, b, c) &= \int_0^\infty \exp\left(\frac{-y}{a}\right) \text{Ei}\left(\frac{-b}{y} - c\right) dy \text{ with } (a > 0, b > 0, c > 0),\end{aligned}$$

where $\text{Ei}(\cdot)$ defined in [22, Eq. (8.221.1)] is the exponential integral function.

Proof: The proof is given in Appendix B. ■

B. P_{TX} is far from the secondary network

We denote $\hat{\mathcal{A}} = \frac{\gamma_B\alpha}{K} \sum_{k=1}^K \sum_{n=1}^N |h_{B_{n,k}S_s}|^2$. The SNR at D can be rewritten as

$$\Psi_D^{FP} = \min\left(\hat{\mathcal{A}}, \frac{\gamma_{\mathcal{I}_p}}{\mathcal{B}}\right) \mathcal{Z}. \quad (22)$$

The PDF of $\hat{\mathcal{A}}$ is given as

$$f_{\hat{\mathcal{A}}}(x) = \left(\frac{K}{\alpha\gamma_B\Omega_{BS}}\right)^{KN} \frac{x^{KN-1}}{\Gamma(KN)} \exp\left(\frac{-Kx}{\alpha\gamma_B\Omega_{BS}}\right) \quad (23)$$

Proof: The PDF of $\hat{\mathcal{A}}$ can be calculated similarly to the PDF of \mathcal{A} by using moment generating function and inverse Laplace transform (see the Appendix A). ■

From (15), (19), and (23), we have the following lemma.

Lemma 2: The OP of the secondary network without neighbouring P_{TX} is given as follows:

$$\begin{aligned}\mathbb{P}_{\text{out}}^{FP} &= 1 - \sum_{m=1}^M \binom{M}{m} (-1)^{m+1} 2\varepsilon \left(\frac{m\beta\alpha\gamma_B\Omega_{BS}}{K\Omega_{SD}}\right)^{\frac{NK}{2}} K_{NK} \left(2\sqrt{\frac{mK\beta}{\Omega_{SD}\alpha\gamma_B\Omega_{BS}}}\right) \\ &\quad - \sum_{m=1}^M \binom{M}{m} \frac{(-1)^m 2\varepsilon m\beta\Omega_{SP_{RX}}}{m\beta\Omega_{SP_{RX}} + \gamma_{\mathcal{I}_p}\Omega_{SD}} \left(\frac{(m\beta\Omega_{SP_{RX}} + \Omega_{SD}\gamma_{\mathcal{I}_p})\alpha\gamma_B\Omega_{BS}}{K\Omega_{SD}\Omega_{SP_{RX}}}\right)^{\frac{NK}{2}} \\ &\quad \times K_{NK} \left(2\sqrt{\frac{(m\beta\Omega_{SP_{RX}} + \Omega_{SD}\gamma_{\mathcal{I}_p})K}{\gamma_B\alpha\Omega_{BS}\Omega_{SD}\Omega_{SP_{RX}}}}\right),\end{aligned} \quad (24)$$

where $\varepsilon = \left(\frac{K}{\alpha\gamma_B\Omega_{BS}}\right)^{KN} \frac{1}{\Gamma(KN)}$.

Proof: The proof is given in Appendix C. ■

IV. ASYMPTOTIC ANALYSIS

In this section, asymptotic expressions of OP in the two scenarios are derived to provide important insights of the considered system. To derive the asymptotic expressions, B_n is considered to have high transmit power to perform beamforming to the selected S_s . As a result, the asymptotic OP of the considered system in the far P_{TX} and near P_{TX} scenarios are respectively given as

$$\begin{aligned} \mathbb{P}_{\text{out}}^{\text{NP}} \stackrel{\text{high } \gamma_B}{\approx} 1 - \sum_{m=1}^M \binom{M}{m} (-1)^m \frac{\gamma_{\mathcal{I}_p} \Omega_{SD}}{\gamma_P \Omega_{P_{TX}D} \Omega_{SP_{RX}} m \beta} \exp \left(\frac{1}{\gamma_P \Omega_{P_{TX}D}} \left[1 + \frac{\gamma_{\mathcal{I}_p} \Omega_{SD}}{\Omega_{SP_{RX}} \beta m} \right] \right) \\ \times \text{Ei} \left(\frac{-1}{\gamma_P \Omega_{P_{TX}D}} \left[1 + \frac{\gamma_{\mathcal{I}_p} \Omega_{SD}}{\Omega_{SP_{RX}} \beta m} \right] \right), \end{aligned} \quad (25)$$

$$\mathbb{P}_{\text{out}}^{\text{FP}} \stackrel{\text{high } \gamma_B}{\approx} 1 - \sum_{m=1}^M \binom{M}{m} (-1)^m \frac{\gamma_{\mathcal{I}_p} \Omega_{SD}}{\Omega_{SP_{RX}} \beta m + \gamma_{\mathcal{I}_p} \Omega_{SD}}. \quad (26)$$

Proof: The proof is given in Appendix D. ■

From the asymptotic expressions, it is observed that in the near P_{TX} scenario, when B_n has high transmit power, the secondary network does not take advantage of the primary network's interference. Therefore, the primary network's interference only has harmful effect on the secondary network. Meanwhile, in the far P_{TX} scenario, the performance of the considered system is only restrained by the peak interference constraint of the primary network.

V. NUMERICAL RESULTS

In this section, the simulation results based on Monte Carlo method are provided to verify the accuracy of the above performance analysis. Without loss of generality, the following parameters are fixed throughout this section $\eta = 0.8$ and $K = 3$.

Fig. 3 reveals the effect of P_{TX} and the number of power beacons on the secondary network. In this figure, $\gamma_P = 20$ dB, $\gamma_{\mathcal{I}_p} = 10$ dB, the number of power beacons is varied from $N = 1$ to $N = 3$, $M = 3$, $\tau = 0.6$, and OP is the function of γ_B . As γ_B increases, the transmit power of S_s increases, followed by a reduction in the OP. Although S_s can create huge transmit power in the transmission phase when γ_B goes large, its transmit power is limited by \mathcal{I}_p . In near P_{TX} scenario, D receives interference from P_{TX} which results in a higher OP than that in the far P_{TX} scenario. In addition, we also observe that increasing the number of power beacons N can provide higher amount of energy to S_s which leads to a decrease in the OP in both scenarios.

In Fig. 4, the impact of the peak interference constraint \mathcal{I}_p at the primary receiver on the OP of secondary network in both near and far P_{TX} scenarios is demonstrated. In this figure, $\gamma_P = 20$ dB, $\gamma_{\mathcal{I}_p} = 10$ and 12 dB, $N = 3$, $M = 3$, $\tau = 0.6$, and OP is the function of γ_B . As the peak interference constraint at the primary receiver is relaxed, the secondary transmitter can transmit with higher transmit power to improve the secondary network performance.

In Fig. 5, the OP of the considered system in the near P_{TX} scenario is plotted as a function of γ_P with a variation in the number of the secondary transmitters. γ_B is fixed at 20 dB, $\gamma_{\mathcal{I}_p} = 20$ dB, $\tau = 0.6$, and $N = 3$. In the near P_{TX} scenario, S_s benefits from the energy harvested from P_{TX} . However, D is impacted by the interference from the P_{TX} . When the transmit power at S_s is limited by \mathcal{I}_p , increasing γ_P will result in high interference at D, followed by an increase in the OP. The figure also shows that, increasing the number of secondary transmitters can reduce the outage probability of the secondary network. The benefit of increasing the number of secondary transmitters in the far P_{TX} scenario can be witnessed in Fig. 6.

In Fig. 7, the effect of EH time on the OP of the considered system is demonstrated. On one hand, if the EH time is short (small τ), S_s will not have enough energy to efficiently transmit its information to the destination, followed by an increase in the OP. On the other hand, if the EH time is long (large τ), the transmission time between S_s and the destination will be shortened which results in a reduction in the capacity of the considered system. Therefore, EH time at S_s should be carefully designed to enhance the performance of the considered system. As in Fig. 7, optimal value of τ for the considered system can be selected in the range of 0.6 to 0.7.

VI. CONCLUSIONS

In this paper, the impact of the primary network on the secondary network in EH-CR networks is investigated. In particular, a secondary transmitter is selected from multiple secondary transmitters based on the CSI of secondary network to transmit information to the secondary receiver. This secondary transmitter is powered by the energy harvested from beamformed power signals of multiple multi-antenna power beacons and power signal from the primary transmitter. To examine the influence of the primary network's interference on the secondary receiver, two scenarios of primary transmitter's locations are considered, i.e., near primary transmitter and far primary transmitter. The analytical and asymptotic expressions of the OP of the considered system in these two scenarios are derived. The results reveal that the appearance of the primary transmitter has negative effects on the secondary network performance. Despite the fact that the

secondary transmitter can harvest energy from the primary transmitter, the secondary receiver suffers from the primary transmitter's interference, followed by a suppression in the secondary network transmission. In addition, although the secondary transmitters can be wireless powered by power sources, the peak interference constraint at the primary receiver limits this advantage. However, increasing the number of power beacons and primary transmitters can effectively improve the performance of the secondary network. Finally, the numerical results were provided to validate our correctness.

APPENDIX A

PROOF OF $f_{\mathcal{A}}(x)$

Recall from (13), \mathcal{A} is expressed as

$$\mathcal{A} = \frac{\gamma_B \alpha}{K} \sum_{n=1}^N \sum_{k=1}^K |h_{B_{n,k}} s_s|^2 + \gamma_P \alpha |h_{P_{TX}} s_s|^2.$$

Because $|h_{B_{n,k}} s_s|^2$ is an exponential random variable, $\sum_{k=1}^K |h_{B_{n,k}} s_s|^2$ follows gamma distribution.

We denote $\mathcal{C}_n = \sum_{k=1}^K \frac{\gamma_B \alpha}{K} |h_{B_{n,k}} s_s|^2$ and $\mathcal{D} = \gamma_P \alpha |h_{P_{TX}} s_s|^2$. Therefore, $\mathcal{C}_n \sim \Gamma(K, \frac{\gamma_B \alpha \Omega_{BS}}{K})$ and $\mathcal{D} \sim \text{Exp}(\gamma_P \alpha \Omega_{P_{TX}} s_s)$. \mathcal{A} can be rewritten as follows:

$$\mathcal{A} = \sum_{n=1}^N \mathcal{C}_n + \mathcal{D}. \quad (\text{A.1})$$

To find PDF of \mathcal{A} , we find the moment generating function (MGF) of \mathcal{A} first. The MGF of \mathcal{C}_n and \mathcal{D} are obtained respectively as follows:

$$M_{\mathcal{C}_n} \{t\} = \left(1 + \frac{\gamma_B \alpha \Omega_{BS} t}{K}\right)^{-KN} \quad (\text{A.2})$$

$$M_{\mathcal{D}} \{t\} = (1 + \gamma_P \alpha \Omega_{P_{TX}} s t)^{-1} \quad (\text{A.3})$$

The MGF of \mathcal{A} is given as

$$M_{\mathcal{A}} \{t\} = \left(1 + \frac{\gamma_B \alpha \Omega_{BS} t}{K}\right)^{-KN} (1 + \gamma_P \alpha \Omega_{P_{TX}} s t)^{-1}. \quad (\text{A.4})$$

From (A.4), after expanding in partial fractions and applying the inverse Laplace transform, we have the PDF of \mathcal{A} as in (20).

APPENDIX B

PROOF OF LEMMA 1

From (12) and (14), the OP of the secondary network with neighbouring P_{TX} can be written as

$$\mathbb{P}_{\text{out}}^{\text{NP}} = \mathbb{P} \left\{ \frac{\min(\mathcal{A}, \frac{\gamma_{\mathcal{I}_p}}{\mathcal{B}}) \mathcal{Z}}{1 + \mathcal{Y}} < \beta \right\} = \mathbb{P} \left\{ \mathcal{Z} < \frac{\beta(1 + \mathcal{Y})}{\min(\mathcal{A}, \frac{\gamma_{\mathcal{I}_p}}{\mathcal{B}})} \right\}. \quad (\text{B.1})$$

To simplify the calculation process, we denote $\mathcal{U} = \min(\mathcal{A}, \frac{\gamma_{\mathcal{I}_p}}{\mathcal{B}})$ and calculate the OP conditioned on \mathcal{U} first.

$$\begin{aligned} \mathbb{P}_{\text{out}|\mathcal{U}}^{\text{NP}} &= \int_0^\infty F_{\mathcal{Z}|\mathcal{U}} \left(\frac{\beta[1 + \mathcal{Y}]}{\mathcal{U}} \right) f_{\mathcal{Y}}(y) dy \\ &= 1 - \sum_{m=1}^M \binom{M}{m} \frac{(-1)^{m+1} \Omega_{\text{SD}} \mathcal{U}}{m\beta\gamma_{\text{P}}\Omega_{\text{P}_{\text{TXD}}} + \Omega_{\text{SD}} \mathcal{U}} \exp \left(\frac{-m\beta}{\Omega_{\text{SD}} \mathcal{U}} \right) \end{aligned} \quad (\text{B.2})$$

\mathcal{U} can be rewritten as

$$\mathcal{U} = \begin{cases} \mathcal{A}, & \text{if } \mathcal{B} < \frac{\gamma_{\mathcal{I}_p}}{\mathcal{A}} \\ \frac{\gamma_{\mathcal{I}_p}}{\mathcal{B}}, & \text{if } \mathcal{B} > \frac{\gamma_{\mathcal{I}_p}}{\mathcal{A}}. \end{cases} \quad (\text{B.3})$$

Plugging (B.3) into (B.2) and calculating the integral conditioned on \mathcal{A} , the OP is given as

$$\begin{aligned} \mathbb{P}_{\text{out}|\mathcal{A}}^{\text{NP}} &= \int_0^{\frac{\gamma_{\mathcal{I}_p}}{\mathcal{A}}} \left[1 - \sum_{m=1}^M \binom{M}{m} \frac{(-1)^{m+1} \Omega_{\text{SD}} \mathcal{A}}{m\beta\gamma_{\text{P}}\Omega_{\text{P}_{\text{TXD}}} + \Omega_{\text{SD}} \mathcal{A}} \exp \left(\frac{-m\beta}{\Omega_{\text{SD}} \mathcal{A}} \right) \right] f_{\mathcal{B}}(y) dy \\ &\quad + \int_{\frac{\gamma_{\mathcal{I}_p}}{\mathcal{A}}}^\infty \left[1 - \sum_{m=1}^M \binom{M}{m} \frac{(-1)^{m+1} \Omega_{\text{SD}} \gamma_{\mathcal{I}_p}}{m\beta\gamma_{\text{P}}\Omega_{\text{P}_{\text{TXD}}} y + \Omega_{\text{SD}} \gamma_{\mathcal{I}_p}} \exp \left(\frac{-m\beta y}{\Omega_{\text{SD}} \gamma_{\mathcal{I}_p}} \right) \right] f_{\mathcal{B}}(y) dy \\ &= 1 - \sum_{m=1}^M \binom{M}{m} (-1)^{m+1} \exp \left(\frac{-m\beta}{\Omega_{\text{SD}} \mathcal{A}} \right) \frac{\Omega_{\text{SD}} \mathcal{A}}{m\gamma_{\text{P}}\Omega_{\text{P}_{\text{TXD}}} \beta + \Omega_{\text{SD}} \mathcal{A}} \\ &\quad - \sum_{m=1}^M \binom{M}{m} (-1)^m \exp \left(\frac{-m\beta}{\Omega_{\text{SD}} \mathcal{A}} - \frac{\gamma_{\mathcal{I}_p}}{\mathcal{A} \Omega_{\text{SP}_{\text{RX}}}} \right) \frac{\Omega_{\text{SD}} \mathcal{A}}{m\gamma_{\text{P}}\Omega_{\text{P}_{\text{TXD}}} \beta + \Omega_{\text{SD}} \mathcal{A}} \\ &\quad - \sum_{m=1}^M \binom{M}{m} (-1)^m \frac{\gamma_{\mathcal{I}_p} \Omega_{\text{SD}}}{m\gamma_{\text{P}}\Omega_{\text{SP}_{\text{RX}}} \Omega_{\text{P}_{\text{TXD}}} \beta} \exp \left(\frac{m\beta \Omega_{\text{SP}_{\text{RX}}} + \gamma_{\mathcal{I}_p} \Omega_{\text{SD}}}{m\gamma_{\text{P}}\Omega_{\text{SP}_{\text{RX}}} \Omega_{\text{P}_{\text{TXD}}} \beta} \right) \\ &\quad \times \text{Ei} \left[-\frac{m\beta \Omega_{\text{SP}_{\text{RX}}} + \gamma_{\mathcal{I}_p} \Omega_{\text{SD}}}{\gamma_{\mathcal{I}_p} \Omega_{\text{SD}} \Omega_{\text{SP}_{\text{RX}}} \left(\frac{\gamma_{\mathcal{I}_p}}{\mathcal{A}} + \frac{\gamma_{\mathcal{I}_p} \Omega_{\text{SD}}}{m\gamma_{\text{P}}\Omega_{\text{P}_{\text{TXD}}} \beta} \right) \right]. \end{aligned} \quad (\text{B.4})$$

(B.4) is obtained with the help of [22, Eq. (3.352.2)]. From (B.4), the OP is formulated as

$$\begin{aligned}
\mathbb{P}_{\text{out}}^{\text{NP}} &= \int_0^\infty \mathbb{P}_{\text{out}|\mathcal{A}} f_{\mathcal{A}}(y) dy \\
&= 1 - \underbrace{\int_0^\infty \sum_{m=1}^M \binom{M}{m} (-1)^{m+1} \exp\left(\frac{-m\beta}{\Omega_{\text{SD}} y}\right) \left(1 - \frac{\varrho_m}{\varrho_m + y}\right) f_{\mathcal{A}}(y) dy}_{Q_1} \\
&\quad - \underbrace{\int_0^\infty \sum_{m=1}^M \binom{M}{m} (-1)^m \exp\left(\frac{-\vartheta_m}{y}\right) \left(1 - \frac{\varrho_m}{\varrho_m + y}\right) f_{\mathcal{A}}(y) dy}_{Q_2} \\
&\quad - \underbrace{\int_0^\infty \sum_{m=1}^M \binom{M}{m} (-1)^m \frac{\gamma_{\mathcal{I}_p} \Omega_{\text{SD}} \exp(\varsigma_m)}{m \gamma_{\text{P}} \Omega_{\text{SP}_{\text{RX}}} \Omega_{\text{P}_{\text{TXD}}} \beta} \text{Ei}\left(\frac{-\varsigma_m \gamma_{\mathcal{I}_p}}{\mathcal{A}} - \frac{\varsigma_m \gamma_{\mathcal{I}_p} \Omega_{\text{SD}}}{m \gamma_{\text{P}} \Omega_{\text{P}_{\text{TXD}}} \beta}\right) f_{\mathcal{A}}(y) dy}_{Q_3}, \quad (\text{B.5})
\end{aligned}$$

where $\varrho_m = \frac{m \gamma_{\text{P}} \Omega_{\text{P}_{\text{TXS}}} \beta}{\Omega_{\text{SD}}}$, $\vartheta_m = \frac{m\beta}{\Omega_{\text{SD}}} + \frac{\gamma_{\mathcal{I}_p}}{\Omega_{\text{SP}_{\text{RX}}}}$, and $\varsigma_m = \frac{m\beta \Omega_{\text{SP}_{\text{RX}}} + \gamma_{\mathcal{I}_p} \Omega_{\text{SD}}}{\gamma_{\mathcal{I}_p} \Omega_{\text{SD}} \Omega_{\text{SP}_{\text{RX}}}}$. Q_1 can be calculated as follows:

$$\begin{aligned}
Q_1 &= \underbrace{\int_0^\infty \sum_{m=1}^M \sum_{l=1}^{KN} \binom{M}{m} (-1)^{m+1} \kappa_{1l} y^{l-1} \exp\left(\frac{-m\beta}{\Omega_{\text{SD}} y} - \frac{Ky}{\gamma_{\text{B}} \alpha \Omega_{\text{BS}}}\right) dy}_{Q_{11}} \\
&\quad + \underbrace{\int_0^\infty \sum_{m=1}^M \binom{M}{m} (-1)^{m+1} \kappa_2 \exp\left(\frac{-m\beta}{\Omega_{\text{SD}} y} - \frac{y}{\gamma_{\text{P}} \alpha \Omega_{\text{P}_{\text{TXS}}}}\right) dy}_{Q_{12}} \\
&\quad + \underbrace{\int_0^\infty \sum_{m=1}^M \sum_{l=1}^{KN} \binom{M}{m} (-1)^m \kappa_{1l} \frac{\varrho_m y^{l-1}}{\varrho_m + y} \exp\left(\frac{-m\beta}{\Omega_{\text{SD}} y} - \frac{Ky}{\gamma_{\text{B}} \alpha \Omega_{\text{BS}}}\right) dy}_{\Theta_1(\beta)} \\
&\quad + \underbrace{\int_0^\infty \sum_{m=1}^M \binom{M}{m} (-1)^m \kappa_2 \frac{\varrho_m}{\varrho_m + y} \exp\left(\frac{-m\beta}{\Omega_{\text{SD}} y} - \frac{y}{\gamma_{\text{P}} \alpha \Omega_{\text{P}_{\text{TXS}}}}\right) dy}_{\Theta_2(\beta)}. \quad (\text{B.6})
\end{aligned}$$

Q_{11} and Q_{12} are given as

$$Q_{11} = \sum_{m=1}^M \sum_{l=1}^{KN} \binom{M}{m} (-1)^{m+1} 2 \kappa_{1l} \left(\frac{m \gamma_{\text{B}} \alpha \beta \Omega_{\text{BS}}}{K \Omega_{\text{SD}}} \right)^{\frac{l}{2}} \text{K}_l \left(2 \sqrt{\frac{m K \beta}{\gamma_{\text{B}} \alpha \Omega_{\text{SD}} \Omega_{\text{BS}}}} \right), \quad (\text{B.7})$$

$$Q_{12} = \sum_{m=1}^M \binom{M}{m} (-1)^{m+1} \kappa_2 2 \sqrt{\frac{m \beta \gamma_{\text{P}} \alpha \Omega_{\text{P}_{\text{TXS}}}}{\Omega_{\text{SD}}}} \text{K}_1 \left(2 \sqrt{\frac{m \beta}{\gamma_{\text{P}} \Omega_{\text{P}_{\text{TXS}}} \Omega_{\text{SD}}}} \right). \quad (\text{B.8})$$

(B.7) and (B.8) are obtained with the help of [22, Eq. (3.471.9)].

Q_2 can be calculated as

$$\begin{aligned}
Q_2 = & \underbrace{\int_0^\infty \sum_{m=1}^M \sum_{l=1}^{KN} \binom{M}{m} (-1)^m \varkappa_{1l} y^{l-1} \exp\left(\frac{-\vartheta_m}{y} - \frac{Ky}{\gamma_B \alpha \Omega_{BS}}\right) dy}_{Q_{21}} \\
& + \underbrace{\int_0^\infty \sum_{m=1}^M \binom{M}{m} (-1)^m \varkappa_2 \exp\left(\frac{-\vartheta_m}{y} - \frac{y}{\gamma_P \alpha \Omega_{P_{TX}S}}\right) dy}_{Q_{22}} \\
& + \underbrace{\int_0^\infty \sum_{m=1}^M \sum_{l=1}^{KN} \binom{M}{m} (-1)^{m+1} \varkappa_{1l} \frac{\varrho_m y^{l-1}}{\varrho_m + y} \exp\left(\frac{-\vartheta_m}{y} - \frac{Ky}{\gamma_B \alpha \Omega_{BS}}\right) dy}_{\Theta_3(\beta)} \\
& + \underbrace{\int_0^\infty \sum_{m=1}^M \binom{M}{m} (-1)^{m+1} \varkappa_2 \frac{\varrho_m}{\varrho_m + y} \exp\left(\frac{-\vartheta_m}{y} - \frac{y}{\gamma_P \alpha \Omega_{P_{TX}S}}\right) dy}_{\Theta_4(\beta)}. \tag{B.9}
\end{aligned}$$

Q_{21} and Q_{22} are given as

$$Q_{21} = \sum_{m=1}^M \sum_{l=1}^{KN} \binom{M}{m} (-1)^m 2 \varkappa_{1l} \left(\vartheta_m \Omega_{BS} \frac{\gamma_B \alpha}{K} \right)^{\frac{l}{2}} K_l \left(2 \sqrt{\frac{K \vartheta_m}{\gamma_B \alpha \Omega_{BS}}} \right) \tag{B.10}$$

$$Q_{22} = \sum_{m=1}^M \binom{M}{m} (-1)^m \varkappa_2 2 \sqrt{\vartheta_m \gamma_P \alpha \Omega_{P_{TX}S}} K_1 \left(2 \sqrt{\frac{\vartheta_m}{\gamma_P \alpha \Omega_{P_{TX}S}}} \right) \tag{B.11}$$

(B.10) and (B.11) are obtained with the help of [22, Eq. (3.471.9)]. From (B.5)-(B.11), we obtain (21).

APPENDIX C

PROOF OF LEMMA 2

From (22), OP of the secondary network without neighbouring P_{TX} is given as

$$\begin{aligned}
\mathbb{P}_{\text{out}}^{\text{FP}} &= \mathbb{P} \left\{ \min \left(\hat{\mathcal{A}}, \frac{\gamma_{\mathcal{I}_p}}{\mathcal{B}} \right) \mathcal{Z} < \beta \right\} \\
&= \int_0^\infty \int_0^\infty \left(1 - \sum_{m=1}^M \binom{M}{m} (-1)^{m+1} \exp \left[\frac{-m\beta}{\Omega_{\text{SD}} \min \left(\hat{\mathcal{A}}, \frac{\gamma_{\mathcal{I}_p}}{\mathcal{B}} \right)} \right] \right) f_{\mathcal{B}}(y) f_{\hat{\mathcal{A}}}(z) dy dz \\
&= 1 - \int_0^\infty \sum_{m=1}^M \binom{M}{m} (-1)^{m+1} \exp \left(\frac{-m\beta}{z\Omega_{\text{SD}}} \right) f_{\hat{\mathcal{A}}}(z) dz \\
&\quad - \int_0^\infty \sum_{m=1}^M \binom{M}{m} (-1)^m \exp \left(\frac{-1}{z} \left[\frac{m\beta}{\Omega_{\text{SD}}} + \frac{\gamma_{\mathcal{I}_p}}{\Omega_{\text{SPRX}}} \right] \right) f_{\hat{\mathcal{A}}}(z) dz \\
&\quad - \int_0^\infty \sum_{m=1}^M \binom{M}{m} (-1)^{m+1} \frac{\gamma_{\mathcal{I}_p} \Omega_{\text{SD}}}{m\beta \Omega_{\text{SPRX}} + \gamma_{\mathcal{I}_p} \Omega_{\text{SD}}} \exp \left(\frac{-1}{z} \left[\frac{m\beta}{\Omega_{\text{SD}}} + \frac{\gamma_{\mathcal{I}_p}}{\Omega_{\text{SPRX}}} \right] \right) f_{\hat{\mathcal{A}}}(z) dz \\
&= 1 - \sum_{m=1}^M \binom{M}{m} (-1)^{m+1} 2\varepsilon \left(\frac{m\beta \alpha \gamma_{\text{B}} \Omega_{\text{BS}}}{K \Omega_{\text{SD}}} \right)^{\frac{NK}{2}} K_{NK} \left(2\sqrt{\frac{mK\beta}{\Omega_{\text{SD}} \alpha \gamma_{\text{B}} \Omega_{\text{BS}}}} \right) \\
&\quad - \sum_{m=1}^M \binom{M}{m} \frac{(-1)^m 2\varepsilon m\beta \Omega_{\text{SPRX}}}{m\beta \Omega_{\text{SPRX}} + \gamma_{\mathcal{I}_p} \Omega_{\text{SD}}} \left(\frac{(m\beta \Omega_{\text{SPRX}} + \Omega_{\text{SD}} \gamma_{\mathcal{I}_p}) \alpha \gamma_{\text{B}} \Omega_{\text{BS}}}{K \Omega_{\text{SD}} \Omega_{\text{SPRX}}} \right)^{\frac{NK}{2}} \\
&\quad \times K_{NK} \left(2\sqrt{\frac{(m\beta \Omega_{\text{SPRX}} + \Omega_{\text{SD}} \gamma_{\mathcal{I}_p}) K}{\gamma_{\text{B}} \alpha \Omega_{\text{BS}} \Omega_{\text{SD}} \Omega_{\text{SPRX}}}} \right), \tag{C.1}
\end{aligned}$$

(C.1) is obtained with the help of [22, Eq. (3.471.9)].

APPENDIX D

PROOF OF ASYMPTOTIC EXPRESSIONS

When the transmit power at B_n is high, from (B.1), the OP of the considered system in the near P_{TX} scenario is formulated as

$$\begin{aligned}
 \mathbb{P}_{\text{out}}^{\text{NP}} &= \mathbb{P} \left\{ \frac{\min \left(\mathcal{A}, \frac{\gamma_{\mathcal{I}_p}}{\mathcal{B}} \right) \mathcal{Z}}{1 + \mathcal{Y}} < \beta \right\} \stackrel{\text{high } \gamma_B}{\approx} \mathbb{P} \left\{ \mathcal{Z} < \frac{\beta \mathcal{B}(1 + \mathcal{Y})}{\gamma_{\mathcal{I}_p}} \right\} \\
 &= \int_0^\infty \int_0^\infty F_{\mathcal{Z}} \left(\frac{\beta x(1 + y)}{\gamma_{\mathcal{I}_p}} \right) f_{\mathcal{B}}(x) f_{\mathcal{Y}}(y) dx dy \\
 &= 1 - \sum_{m=1}^M \binom{M}{m} (-1)^m \frac{\gamma_{\mathcal{I}_p} \Omega_{\text{SD}}}{\gamma_P \Omega_{P_{TX}D} \Omega_{\text{SP}_{RX}} m \beta} \exp \left(\frac{1}{\gamma_P \Omega_{P_{TX}D}} \left[1 + \frac{\gamma_{\mathcal{I}_p} \Omega_{\text{SD}}}{\Omega_{\text{SP}_{RX}} \beta m} \right] \right) \\
 &\quad \times \text{Ei} \left(\frac{-1}{\gamma_P \Omega_{P_{TX}D}} \left[1 + \frac{\gamma_{\mathcal{I}_p} \Omega_{\text{SD}}}{\Omega_{\text{SP}_{RX}} \beta m} \right] \right). \tag{D.1}
 \end{aligned}$$

(D.1) is obtained with the help of [22, Eq. (3.352.4)]. Similarly, from (C.1), the OP of the considered system in the far P_{TX} scenario is formulated as

$$\begin{aligned}
 \mathbb{P}_{\text{out}}^{\text{FP}} &= \mathbb{P} \left\{ \min \left(\hat{\mathcal{A}}, \frac{\gamma_{\mathcal{I}_p}}{\mathcal{B}} \right) \mathcal{Z} < \beta \right\} \stackrel{\text{high } \gamma_B}{\approx} \mathbb{P} \left\{ \mathcal{Z} < \frac{\beta \mathcal{B}}{\gamma_{\mathcal{I}_p}} \right\} \\
 &= \int_0^\infty F_{\mathcal{Z}} \left(\frac{\beta \mathcal{B}}{\gamma_{\mathcal{I}_p}} \right) f_{\mathcal{B}}(x) dx \\
 &= 1 - \sum_{m=1}^M \binom{M}{m} (-1)^m \frac{\gamma_{\mathcal{I}_p} \Omega_{\text{SD}}}{\Omega_{\text{SP}_{RX}} \beta m + \gamma_{\mathcal{I}_p} \Omega_{\text{SD}}}. \tag{D.2}
 \end{aligned}$$

REFERENCES

- [1] Z. Hadzi-Velkov, I. Nikoloska, G. K. Karagiannidis, and T. Q. Duong, “Wireless networks with energy harvesting and power transfer: Joint power and time allocation,” *IEEE Signal Process. Lett.*, vol. 23, no. 1, pp. 50–54, Jan. 2016.
- [2] Z. Hadzi-Velkov, N. Zlatanov, T. Q. Duong, and R. Schober, “Rate maximization of decode-and-forward relaying systems with RF energy harvesting,” *IEEE Commun. Lett.*, vol. 19, no. 12, pp. 2290–2293, Dec. 2015.
- [3] Y. Liu, L. Wang, S. A. Raza Zaidi, M. Elkashlan, and T. Q. Duong, “Secure D2D communication in large-scale cognitive cellular networks: A wireless power transfer model,” *IEEE Trans. Commun.*, vol. 64, no. 1, pp. 329–342, Jan. 2016.
- [4] J. G. Andrews, S. Buzzi, W. Choi, S. V. Hanly, A. Lozano, A. C. K. Soong, and J. C. Zhang, “What will 5G be?” *IEEE J. Sel. Areas Commun.*, vol. 32, no. 6, pp. 1065–1082, Jun. 2014.
- [5] E. Larsson, O. Edfors, F. Tufvesson, and T. Marzetta, “Massive MIMO for next generation wireless systems,” *IEEE Commun. Mag.*, vol. 52, no. 2, pp. 186–195, Feb. 2014.
- [6] P. Wang, Y. Li, L. Song, and B. Vucetic, “Multi-gigabit millimeter wave wireless communications for 5G: From fixed access to cellular networks,” *IEEE Commun. Mag.*, vol. 53, no. 1, pp. 168–178, Jan. 2015.
- [7] K. Huang and X. Zhou, “Cutting the last wires for mobile communications by microwave power transfer,” *IEEE Commun. Mag.*, vol. 53, no. 6, pp. 86–93, Jun. 2015.

- [8] K. Huang and V. K. N. Lau, "Enabling wireless power transfer in cellular networks: architecture, modeling and deployment," *IEEE Trans. Wireless Commun.*, vol. 13, no. 2, pp. 902–912, Feb. 2014.
- [9] X. Zhou, R. Zhang, and C. K. Ho, "Wireless information and power transfer: Architecture design and rate-energy tradeoff," *IEEE Trans. Commun.*, vol. 61, no. 11, pp. 4754–4767, Nov. 2013.
- [10] A. A. Nasir, X. Zhou, S. Durrani, and R. A. Kennedy, "Relaying protocols for wireless energy harvesting and information processing," *IEEE Trans. Wireless Commun.*, vol. 12, no. 7, pp. 3622–3636, Jul. 2013.
- [11] S. Lee, R. Zhang, and K. Huang, "Opportunistic wireless energy harvesting in cognitive radio networks," *IEEE Trans. Wireless Commun.*, vol. 12, no. 9, pp. 4788–4799, Sep. 2013.
- [12] H. Ju and R. Zhang, "Throughput maximization in wireless powered communication networks," *IEEE Trans. Wireless Commun.*, vol. 13, no. 1, pp. 418–428, Jan. 2014.
- [13] A. A. Nasir, X. Zhou, S. Durrani, and R. A. Kennedy, "Wireless-powered relays in cooperative communications: Time-switching relaying protocols and throughput analysis," *IEEE Trans. Commun.*, vol. 63, no. 5, pp. 1607–1622, May 2015.
- [14] Federal Communications Commission, *Spectrum Policy Task Force Report*. ET Docket No. 02-155, 2002.
- [15] J. Mitola and G. Q. Maguire, "Cognitive radio: Making software radios more personal," *IEEE Pers. Commun.*, vol. 6, no. 4, pp. 13–18, Aug. 1999.
- [16] Y. Liu, L. Wang, T. T. Duy, M. El Kashlan, and T. Q. Duong, "Relay selection for security enhancement in cognitive relay networks," *IEEE Wireless Commun. Lett.*, vol. 4, no. 1, pp. 46–49, Feb. 2015.
- [17] T. T. Duy, G. C. Alexandropoulos, V. T. Tung, V. N. Son, and T. Q. Duong, "Outage performance of cognitive cooperative networks with relay selection over double-Rayleigh fading channels," *IET Communications*, vol. 10, no. 1, pp. 57–64, Jan. 2016.
- [18] A. Goldsmith, S. Jafar, I. Maric, and S. Srinivasa, "Breaking spectrum gridlock with cognitive radios: An information theoretic perspective," *Proc. IEEE*, vol. 97, no. 5, pp. 894–914, May 2009.
- [19] M. Pratibha, K. H. Li, and K. C. Teh, "Channel selection in multichannel cognitive radio systems employing RF energy harvesting," *IEEE Trans. Veh. Technol.*, vol. 65, no. 1, pp. 457–462, Jan. 2016.
- [20] S. Yin, E. Zhang, Z. Qu, L. Yin, and S. Li, "Optimal cooperation strategy in cognitive radio systems with energy harvesting," *IEEE Trans. Wireless Commun.*, vol. 13, no. 9, pp. 4693–4707, Sep. 2014.
- [21] P. Pratibha, K. H. Li, and K. C. Teh, "Dynamic cooperative sensing-access policy for energy-harvesting cognitive radio systems," *IEEE Trans. Veh. Technol.*, vol. PP, no. 99, pp. 1–1, 2016.
- [22] I. S. Gradshteyn and I. M. Ryzhik, *Table of integrals, series, and products*, 7th ed. San Diego, CA: Academic press, 2007.

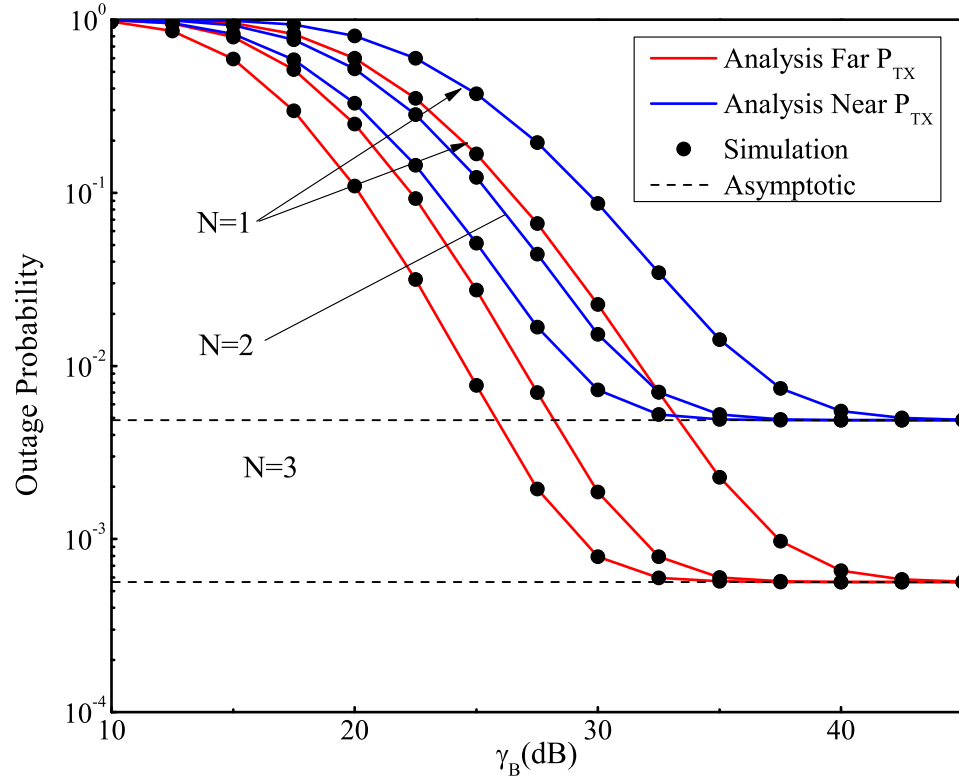


Fig. 3: OP of the considered system in the two scenarios with different numbers of power beacons.

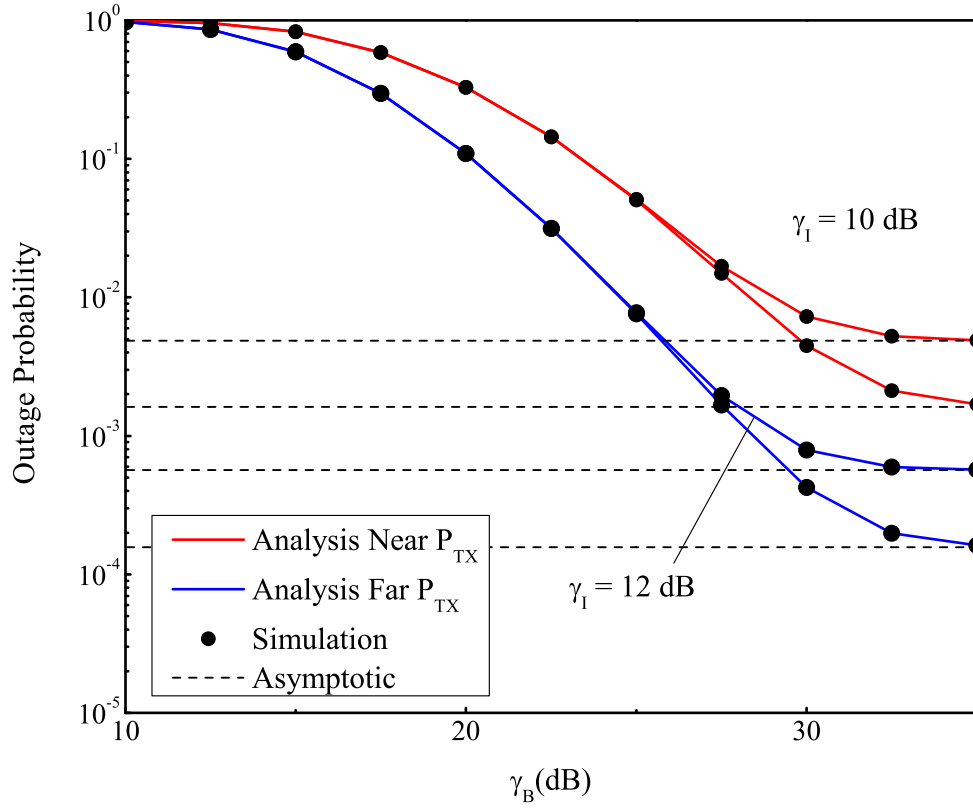


Fig. 4: OP of the considered system in the two scenarios with different values of γ_{I_p} .

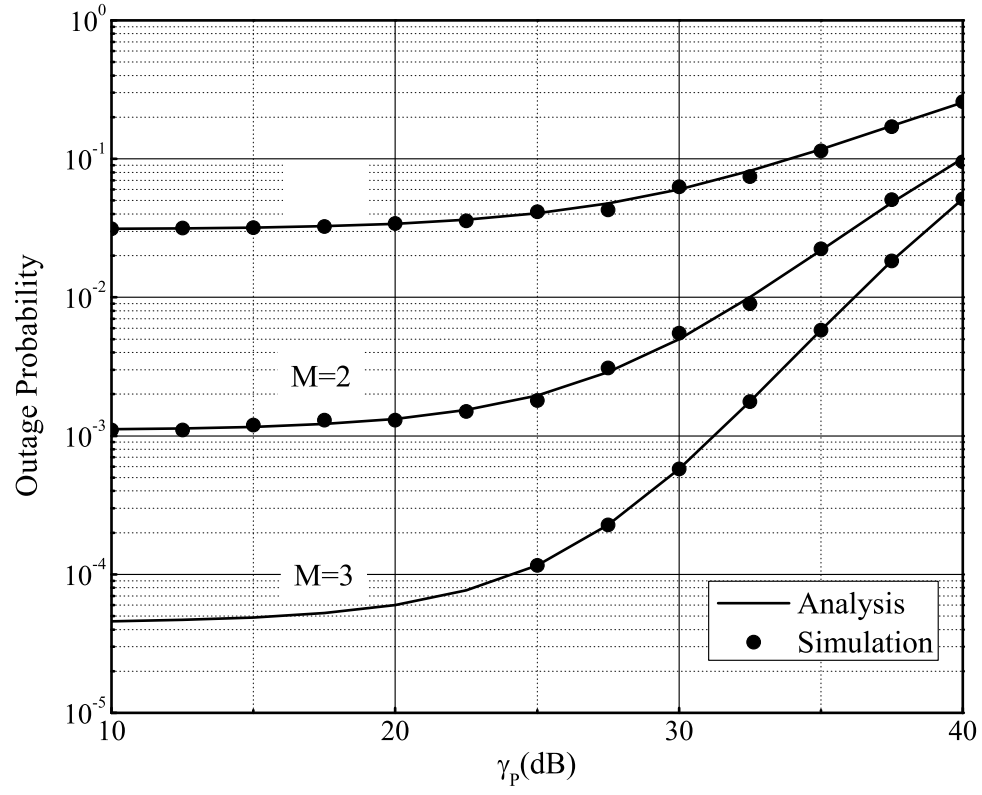


Fig. 5: OP versus γ_p in the near P_{TX} scenario with different numbers of S .

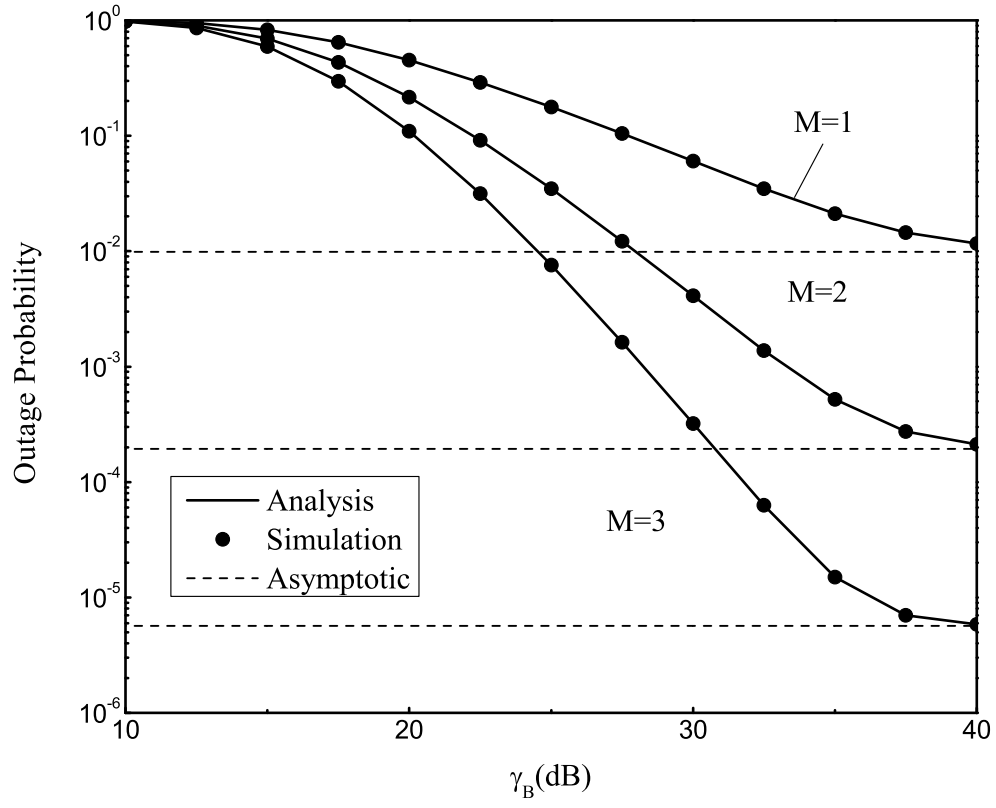


Fig. 6: OP in the far P_{TX} scenario with different numbers of S .

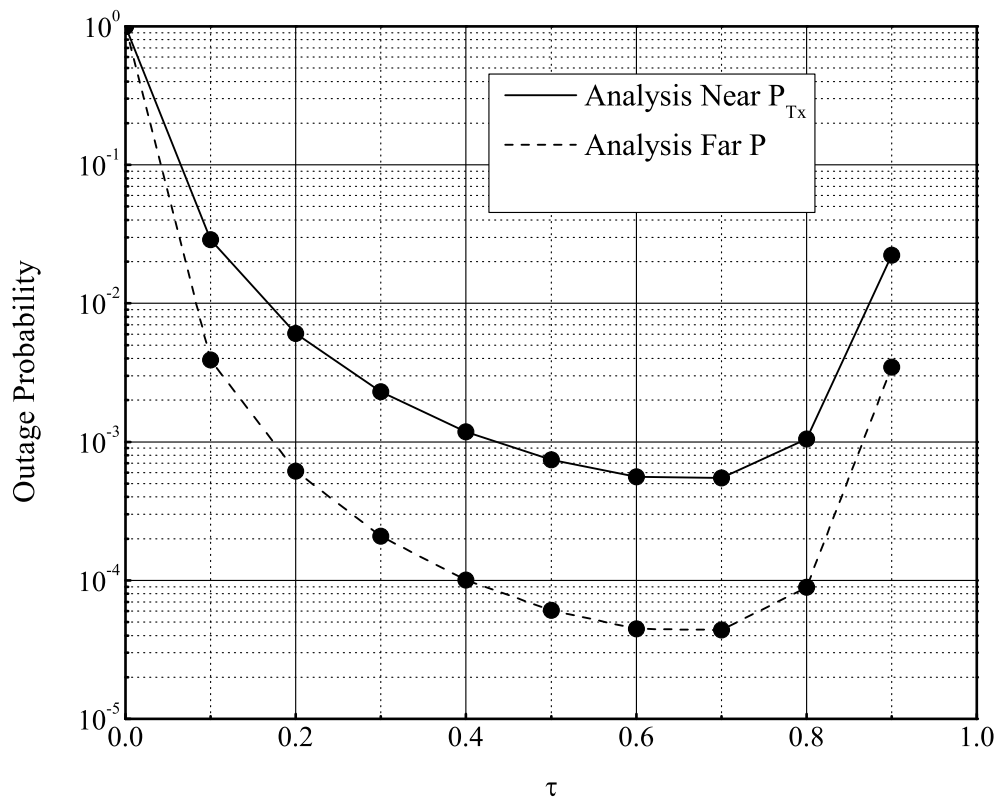


Fig. 7: OP versus τ in the far P_{Tx} and near P_{Tx} scenarios.